Ph.D. Dissertation of Medicine

Molecular subtyping of ependymoma and prognostic impact of Ki-67

뇌실막종의 분자형에 따른 분류와 Ki-67의 예후 예측력

August 2022

Department of Pathology

Graduate School of Medicine

Seoul National University

Ka Young Lim

의학박사 학위논문

Molecular subtyping of ependymoma and prognostic impact of Ki-67

뇌실막종의 분자형에 따른 분류와 Ki-67의 예후 예측력

2022년 8월

서울대학교 대학원

의학과 병리학 전공

임 가 영

Molecular subtyping of ependymoma and prognostic impact of Ki-67

지도교수 박성혜

이 논문을 의학박사 학위논문으로 제출함

2022 년 4 월

서울대학교 대학원

의학과 병리학전공

임 가 영

임 가 영의 의학박사 학위논문을 인준함

2022 년 7 월

위 원 장 김 승 기 (인)

부위원장 박 성 혜 (인)

위 원 정 경 천 (인)

위 원 이 철 (인)

위 원 김 세 훈 (인)

Abstract

Molecular subtyping of ependymoma and prognostic impact of Ki-67

Ka Young Lim

Department of Pathology

Graduate School of Medicine

Seoul National University

Although ependymomas (EPNs) have similar histopathology, they are heterogeneous tumors with diverse immunophenotypes, genetics, epigenetics, and different clinical behavior according to anatomical locations. We reclassified 141 primary EPNs from a single institute with immunohistochemistry (IHC) and next-generation sequencing (NGS). Supratentorial (ST), posterior fossa (PF), and spinal (SP) EPNs comprised 12%, 41%, and 47% of our cohort, respectively. Fusion genes were found only in ST-EPNs except for one SP-EPN with ZFTA-YAP1 fusion, NF2 gene alterations were found in SP-EPNs, but no driver gene was present in PF-EPNs. Surrogate IHC markers revealed high concordance rates between L1CAM and ZFTA-fusion and H3K27me3 loss or EZHIP overexpression was used for PFA-EPNs. The 7% cut-off of Ki-67 was sufficient to classify EPNs into two-tiered grades at all anatomical

locations. Multivariate analysis also delineated that a Ki-67 index was the only independent prognostic factor in both overall and progression-free survivals. The gain of chromosome 1q and CDKN2A/2B deletion were associated with poor outcomes, such as multiple recurrences or extracranial metastases. In this study, we propose a cost-effective schematic diagnostic flow of EPNs by the anatomical location, three biomarkers (L1CAM, H3K27me3, and EZHIP), and a cut-off of a 7% Ki-67 labeling index.

Keywords: ependymoma, genetics, epigenetics, Ki-67, L1CAM, H3K27me3, EZHIP, *ZFTA*, *c11orf95, YAP1*

Student Number: 2019-36666

초록

뇌실막종(ependymomas, EPNs)은 유사한 조직형을 가지고 있지만, 해부학적 위치, 면역표현형, 유전학, 후성유전학적 특성에 따라 다양한 임상 양상을 보이는 종양이다. 본 연구에서는 면역조직화학 및 차세대 염기서열분석(NGS)을 사용하여 단일 기관에서 141 례의 뇌실막종을 재분류하였다. 천막상(ST: supratentorial), 후와(PF: posterior fossa) 및 척수(SP: spinal) 뇌실막종은 각각 우리 코호트의 12%, 41% 및 47%를 차지하였다. 융합 유전자는 *ZFTA-YAP1* 융합이 있는 척수뇌실막종 1 례를 제외하고 천막상뇌실막종에서만 발견되었으며, NF2 유전자 돌연변이는 척수뇌실막종에서 발견되었다. 이미 알려진 바와 같이 후와뇌실막종에서는 드라이버 돌연변이는 발견되지 않았다. 면역 마커인 L1CAM 양성과 ZFTA-융합 사이에서는 높은 일치율이 관찰되어 L1CAM 은 ZFTA-융합을 예측하는 좋은 면역 마커임을 확인했다. 후두 A 형-뇌실막종은 H3K27me3 소실 또는 EZHIP 과발현의 면역표현형을 보였으며 이 두 개의 마커는 서로간 높은 상관관계를 보였다. 뇌실막종의 모든 해부학적 위치에서 Ki-67 의 7% 컷오프는 두개의 등급으로 분류하기에 충분한 기준임을 발견하였다. 또한 다변수 분석을 통해 Ki-67 지수가 전체 생존 및 무진행 생존을 반영하는

유일한 독립적인 예후 인자임을 확인하였다. 염색체 1q 의 증가 및 CDKN2A/2B 결실은 다발성 재발 또는 두개 밖으로의 전이와 같은 불량한 예후와 통계학적으로 의미가 높은 상관관계를 보였다. 이러한 연구 결과를 바탕으로, 우리는 해부학적 위치, 3 개의 바이오 마커인 L1CAM, H3K27me3 및 EZHIP 및 Ki-67 표지 지수의 7% 컷오프를 이용하는 뇌실막종의 효율적인 도식적 진단 흐름을 제안한다.

주요어: 뇌실막종, 유전학, 후성유전학, Ki-67, L1CAM, H3K27me3, EZHIP, *ZFTA*, *c11orf95, YAP1*

학번: 2019-36666

CONTENTS

LIST OF ABBREVIATIONS

EPN, ependymoma

CNS, central nervous system

ST, supratentorial

PF, posterior fossa

SP, spinal

WHO, World Health Organization

MVP, microvascular proliferation

GTR, gross total resection

STR, subtotal resection

RT, radiation therapy

CT, chemotherapy

CCRT, concurrent CT and RT

H3K27me3, trimethylation of lysine 27 of histone H3

CIMP, CpG island methylator phenotype

NF2, neurofibromatosis type 2

OS, overall survival

PFS, progression-free survival

FISH, fluorescent in situ hybridisation

IHC, immunohistochemistry

NGS, next-generation sequencing

WES, whole-exome sequencing

FFPE, formalin-fixed paraffin-embedded

SNV, single nucleotide variant

CNV, copy number variation

NOS, not otherwise specified

GTR, gross total resection

STR, subtotal resection

LIST OF TABLES

LIST OF FIGURES

INTRODUCTION

Background

It has been known that the previous WHO classification of tumors of the central nervous system, mainly based on anatomy and histology, had limitations in reflecting biological behaviors. Thereafter, advances in understanding of the biological basis and molecular characteristics of ependymal tumors prompted the cIMPACT-NOW group to recommend a new classification. It recommended a new taxonomy reflecting molecular alterations and it was adopted in the new 2021 WHO classification of tumors of the central nervous system.

Purpose of this study

We review tumors diagnosed as ependymomas and reclassified them according to the the 2021 WHO classification. We evaluate whether the molecular subtyping of ependymomas well reflect the clinical behavior. We find an additional objective parameter to increase the accuracy in tumor grading. Finally, we suggest a cost-effective diagnostic flow using surrogate markers which will be useful in many clinical fields where molecular laboratories are not well equipped. We identify any exceptional cases in this process which has not been reported.

Definition of ependymomas

Ependymomas (EPNs) are uncommon neuroepithelial malignancies of the central

nervous system (CNS) that can occur in both children and adults [1-3]. They are the third most common CNS tumours in children, arising throughout the entire neuraxis, including the supratentorial (ST), posterior fossa (PF), and spinal (SP) cord [1, 3]. The hypothetical tumour origin is assumed to be the regionally distinct radial glial cells of the ventricle or spinal canal wall [1, 2, 4].

Limitations of previous EPN classification based on histology

The previous World Health Organization (WHO) classification, EPNs are subdivided based mainly on histology and included only one genetically defined EPN subtype, EPN, *RELA* fusion-positive. Histologically defined subtypes include the classic EPN (WHO grade 2) with its three histological subtypes: papillary, clear cell, and tanycytic, anaplastic EPN (WHO grade 3), subependymoma (WHO grade 1), and myxopapillary EPN (WHO grade 2). EPNs have two tier grade, grade 2 and 3, but subependymoma is grade 1 and myxopapillary EPN is grade 2 [1, 5]. However, It has been known that there are pitfalls in EPN grading based on histological parameters, such as mitotic counts and microvascular proliferation, because they lack clear cut criteria for WHO grades 2 and 3 and are limited in that they cannot reflect biological behaviour and patient outcomes [6]. In a 3-phase study conducted by Ellison et al., 229 intracranial ependymomas were reviewed by five pathologists to assess the diagnostic concordance. The allocated grade 2 and grade 3 ranged from 19% to 59% and 41% to 81% respectively [7]. This discrepancy is mainly due to the lack of reproducible criteria to define the anaplastic morphology. This is because the cutoff

of mitosis is unclear and necrosis can be seen in grade 2 as well as grade 3 EPNs. Still, the 2021 WHO criteria described that anaplastic EPNs are characterised by brisk mitoses and microvascular proliferation (MVP), but there was no mention of an exact number that defines the brisk mitoses.

Knowledge improvement in molecular genetics

In recent years, advanced molecular analyses have been implemented to overcome the interobserver variation in diagnosis of CNS tumours and to standardize the diagnostic process. In 2015, Pajtler et al. aimed to establish an uniform classification by DNA methylation profiling and retrieved 500 EPNs of supratentorial, posterior fossa and spinal cord. They reported that EPNs can be subdivided into nine distinct epigenetic subgroups by methylation profiling and annotated the subgroups as followed, based on the anatomical location, histology and molecular alteration: ST-EPN-*ZFTA*, ST-EPN-*YAP1*, ST-SubEPN, PF-EPN-group A, PF-EPN-group B, PF-SubEPN, SP-EPN, SP-SubEPN, and myxopapillary EPN [6].

This taxonomy was adopted in the 2020 cIMPACT-NOW update 7 and the new 2021 WHO classification, reflecting the major molecular alterations and biological behaviours [5].

Two recurrent molecular alterations in ST-EPNs: *ZFTA* fusion and *YAP1* fusion

ST-EPNs are genetically defined two subtypes, which are *zinc 119 finger translocation associated* (*ZFTA*, previous term, *c11orf95*) fusion-positive (WHO

grade 3), previously known as *RELA* fusion before the 2021 WHO classification, and *yes associated protein 1* (*YAP1*) fusion-positive ST-EPNs (WHO grade 2) [8-10].

Molecular mechanism of *ZFTA* fusion and Constitutive NFkB activation

ZFTA fusion accounts for more than 70% of ST-EPNs and shows aggressive clinical behaviour [11, 12]. *ZFTA* partners with a variety of transcriptional co-activators at translocation. The most common fusion occurs between *ZFTA* and *RELA* (approximately 70%), followed by *ZFTA-YAP1* or *ZFTA-Mastermind-like domain containing 1* (*MAMLD1,* previous term *CXorf6)* [13, 14].

A three-step transformation mechanism of *ZFTA* fusion has been reported by Kupp et al., including spontaneous nuclear translocation, chromatin binding and remodelling, and aberrant activation of gene expression [8, 9]. As a result, *ZFTA* fusion proteins act as aberrant transcription factors, results in constitutive nuclear translocation, and drive oncogenic signalling directly, including NF-κB signaling, in EPNs [15, 16].

L1CAM overexpression sustains NFkB pathway

The increased expression of L1CAM, the neural cell adhesion molecule L1, has been known to be correlated with aggressive ovarian, colorectal and pancreatic cancer [17-19] and considered as an important diagnostic marker for cancer progression. The overexpression of L1CAM in cultured pancreatic cancer cells induces sustained NFkB activation. Constitutive NFkB activation can be reversed by depletion of L1CAM via siRNA [20]. The transformation mechanism of *ZFTA*-fusion and

L1CAM-mediated signaling are important for identifying therapeutic targets, given that there are few treatment options other than maximal tumour resection and RT for EPNs.

YAP1 fusion as the recurrent genetic abnormality of low-grade ST-EPNs

YAP1-MAMLD1 fusion is another recurrent genetic abnormality of low-grade ST-EPNs [10, 21]. YAP1 is one of the main downstream effectors of the Hippo signalling pathway which plays a role as a tumor suppressor by regulating cell proliferation and anti-apoptosis. Dysregulation of this pathway results in tissue overgrowth and tumorigenesis and is frequently identified in human cancer [22]. Its significance in biological alterations is not well-known, but it is involved in various tumours including glioma [23], Sonic hedgehog-type medulloblastoma [24] and colon cancer [10, 21].

Different epigenetic signatures of PF-EPNs: PFA-CIMP$^+$ EPNs and PFB-CIMP$^-$ EPNs

PF-EPNs are characterised by no significant somatic mutations, DNA/RNA rearrangements, or copy number abnormalities. Instead, PFA-EPN exhibits loss of broad H3K27me3, but retention of H3K27me3 at CpG islands which is a CpG island methylator phenotype (CIMP) [25, 26]. CpG islands are hypermethylated exclusively in PFA tumours, a pattern that was not detected in PFB-EPNs. In conclusion, PFA-EPNs exhibit a 'CIMP phenotype' and were reffered to as PFA-CIMP$^+$ EPNs, on the

other hand, PFB tumours as PFB-CIMP$^-$ EPNs.

EZHIP inhibits PRC2 activity and induce the global reduction of H3K27me3 in PFA

EZH inhibitory protein (EZHIP; previous nomenclature, *CXorf67*) overexpression have been reported to be found in up to 90% of PFA-EPNs and associated with poor prognosis .EZHIP inhibit PRC2 complex and induce the global reduction of H3K27me3 [27, 28]. Aberrant EZHIP expression plays a role as an oncohistone mimic, which is mutually exclusive from H3K27M mutation [29].

SP-EPNs shows indolent behaviour and different molecular alterations

SP-EPNs are known to have indolent clinical courses. The genetic aberrations of SP-EPNs are quite different from those of intracranial EPNs. *NF2* deletion or mutations or monosomy 22 account for more than 30-50% of SP-EPN cases, but only 4.4% of intracranial EPNs [30, 31]. The upper cervical SP cord is the most frequently affected location in SP-EPN with *NF2* deletion [32].

***MYCN*-amplified SP-EPNs are extremely rare but highly aggressive tumors**

As extremely rare but highly aggressive tumors, the genetically defined *MYCN*-amplified SP-EPNs (WHO grade 3) have been reported [3, 5, 33]. They present multifocal development and early dissemination throughout the neuraxis. Ghasemi et al. reported that overall survival (OS) and progression-free survival (PFS) of SP-EPN-*MYCN* were similar to those of ST-EPN-*ZFTA* or PFA-EPN [34].

Necessity to evaluate prognostic impacts of several variables and to search an objective parameter in segregating grade 2 and grade 3

Over the past decade, unmatched advances have been made in the classification of brain tumours and the discovery of genetic factors, especially in the classification of EPNs. However, clinically, histological grading is still important as the 5 year overall survival of patients with grade 3 EPNs was significantly worse than that of patients with grade 2 EPNs in a large epidemiological study of 1345 patients [35]. In addition, the histological grade is also important for determining the treatment options after surgery. The European Association of Neuro-Oncology has proposed guidelines for the treatment of intracranial EPNs; in both children and adults, and total resection is the treatment of choice. Postoperative local radiation therapy (RT) is recommended in children regardless of the size or tumor grade of the residual tumor, but in adults, postoperative RT is only performed in grade 3 EPN and in grade 2 only if the residual tumor is present [36].

Topics of our study

Here, we reclassified EPNs of our institute for 20 years using the above-mentioned anatomical, genetic, and epigenetic classifiers, known to date as the best taxonomy of EPNs, and report the clinicopathological characteristics and biological behaviour of these subgroups accordingly. We studied the clinical history, pathological features, biological behaviour, and correlation studies, including the correlation between IHC results, such as L1CAM positivity, loss of H3K27me3 and EZHIP overexpression,

and Kaplan-Meier survival analysis of PFS and OS. In addition, we studied the association of copy number variations and clinical outcome. Furthermore, we studied the prognostic impact of clinical and histopathological parameters on intracranial EPNs. We also aimed to suggest a cutoff of the Ki-67 labeling index to separate grades 2 and 3 and finally suggest a cost-effective schematic diagnostic flow of EPNs. In addition, we report a novel discovery; The one is SP-EPN harbouring *ZFTA-YAP1* fusion, which suggests that *ZFTA* fusion is not exclusive to the supratentorial region.

MATERIALS AND METHODS

Patient population

We reviewed the medical records and pathological findings of 223 newly diagnosed EPNs from the archives of Seoul National University Hospital (SNUH) between 2000 and 2020. There were 78 cases excluded due to myxopapillary EPNs (n=19), subependymoma (n=2), recurrent EPNs (n=30), missing paraffin blocks (n=17), suboptimal IHC results by poor block quality (n=12), and diagnosis revision (n=2). IHC and molecular studies successfully reclassified 141 EPNs, including 17 (12%) ST-EPNs, 58 (41%), PF-EPNs, and 66 (47%) SP-EPNs (Fig. 1). Seventy percent of ST-EPNs-ZFTA fusion-positive (Child: 1– to 16-year-old, median: 8-year-old; Adult: 32–51, Median: 41-year-old) and 1 case of ST-EPNs YAP1- MAMLD1 fusion-positive occurred in children (Table 1). Interestingly, all PFA-EPNs occurred in

children (0– to 16-year-old, median: 2.8-year-old), except for one clear cell PFA-EPN, occurring in a 38-year-old woman, while 100% of PFB-EPNs and 89% of SP-EPNs occurred in adults. We reviewed the clinicopathological features and genetic alterations of the EPNs. We analysed the concordance rate of the four IHC surrogate markers, L1CAM and NFkB, with *ZFTA* fusion-positive EPNs and H3K27me3 loss and EZHIP overexpression with PFA-EPNs, and vice versa for PFB-EPNs. We also determined an adequate cutoff of the Ki-67 labeling index to differentiate between grade 2 and grade 3, and compared it with the genetic groups and clinical outcomes.

For survival comparison, we obtained survival data for all 141 patients with EPNs who had been treated at SNUH from 2000 to 2020. Informed consent for the genetic study of brain tumours was obtained from the patients and parents of the children. The institutional review board of our hospital approved this study (approval no.: 2012-034-1179) and was performed under the ethical standards laid down in the 1964 Declaration of Helsinki and its later amendments.

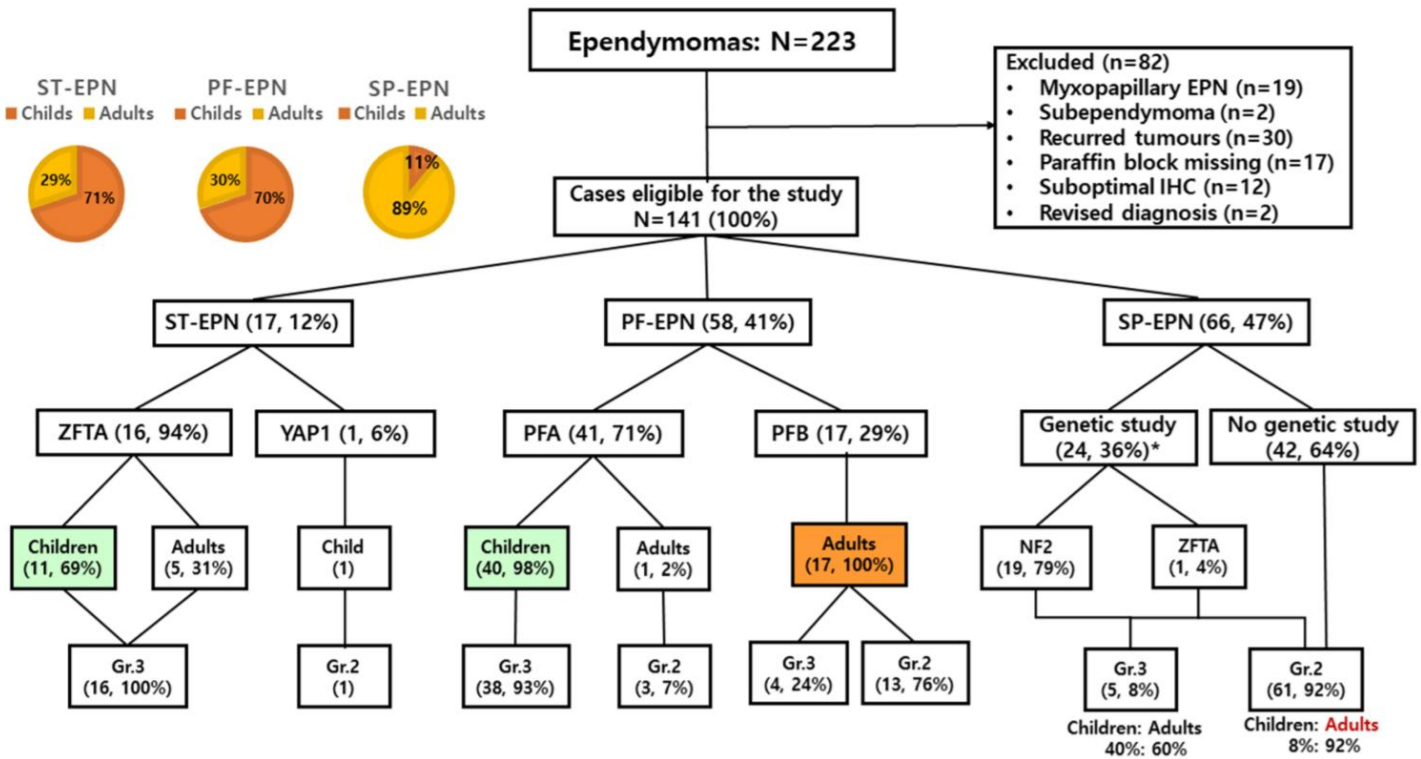

Fig 1. The patients' population in the study. There were a total of 141 EPNs: 17 (12%) ST-EPNs, 58 (41%) PF-EPNs, and 66 (47%) SP-EPNs. This schematic view is the result of the classifcation of our EPNs according to the cIMPACT-NOW update 7

Table 1. Epidemiology of our patients with ST-, PF- and SP-EPNs

Subtype		ST-EPN-*ZFTA* (n=16)	ST-EPN-*YAP1* (n=1)		PFA (n=41)	PFB (n=17)		SP-EPN-Grade 2 (n=61)	SP-EPN-Grade 3 (n=5)
Gender	M: F	5: 3	F (1)		1.6: 1	1: 1.4		1.2: 1	1:4
Age (years)	Total: Median (range) Children Adult	14 (1~51) 8 (1~16) 41 (32~51)	6		3 (0~16)#	41 (21~69)		49 (8~73)	26 (5~49)
Site	Frontal lobe	11*	1	4^{th}V	17	13	C	37	1
	Parietal lobe	4*	-	4^{th}V + 3^{rd}V	1	0	C & T	8	0
	Occipital lobe	1	-	4^{th}V + CPA	1	0	T	11	2
	Temporal lobe	1*	-	Brainstem	2	0	T & L	2	0
	Basal ganglia	2*	-	CMJ	0	1	L	3	2
	Thalamus	2*	-	Cerebellum	10	1			
	Lateral V	1	-	CPA	10	2			
Treatement	GTR only	1	1		4	4		59	1
	GTR + RT	7	-		7	3		-	3
	GTR + CT	1	-					-	
	GTR + CCRT	3	-		12	2		1	1
	STR + RT	1	-		4	5		1	-
	STR + CCRT	3	-		13	2		-	-
	Data missed		-		1	1		-	-
F/U (mo.)	Median (range)	42 (3~99)	99		48 (1~234)	49 (0~139)		37 (0~1003)	8 (0~39)
	No. of dead (%)	3 (19%)	-		15 (37%)	1 (6%)		4 (7%)	0 (0%)
	No. of recur (%)	9 (56%)	-		29 (71%)	4 (24%)		5 (8%)	1 (20%)
Survival (mo.)	OS: Median (range)	42 (3~100)	99		49 (5~234)	55 (0~139)		39 (0~1003)	8 (0~39)
	PFS: Median (range)	23 (0~65)	99		19 (0~216)	48 (0~139)		38 (0~1003)	8 (0~39)

*; In the cases of multiple sites, they were counted twice. V: ventricle, CPA: cerebello-pontine Angle, CMJ: cervicomedullary junction, ST: supratentorial, C: cervical spinal cords, T: thoracic spinal cords, Ls: lumbar spinal cords, F/U: follow up

Pathology and immunohistochemistry

All tumours were reviewed at SNUH by two pathologists (KYL and SHP). Histological features including histologic subtype, necrosis, vascular proliferation, and nuclear pleomorphism were assessed. IHC staining was performed on 4-μm thick formalin-fixed and paraffin-embedded (FFPE) tissues using an automatic immunostaining system (BenchMark ULTRA system; Ventana-Roche, Mannheim, Germany). The primary antibodies used in this study were as follows: mouse monoclonal anti-L1CAM antibody (UJ127, 1:10,000; Millipore, Temecula, USA), rabbit monoclonal anti-NF-κB p65 antibody (D14E12, 1:1000, Cell Signaling, Boston, USA), mouse monoclonal anti-YAP1 antibody (SC-101199, 1:300; Santa Cruz, Texas, USA), rabbit monoclonal H3K27me3 antibody (C36B11, 1:100, Cell Signaling, Boston, USA), rabbit polyclonal anti-CXorf67 antibody (HPA004003, 1:300, Millipore, Temecula, USA), rabbit polyclonal anti-HH3 (K27M) antibody (ABE419, 1:1000, Millipore, Temecula, USA), mouse monoclonal anti-Ki-67 antibody (M7240, 1:100; Dako, Glostrup, Denmark) (Table 2). Morphometric analysis was performed to count the Ki-67 index using the AperioSpectrumPlus n9 algorithm (Leica Biosystems, Wetzlar, Germany) or the Sectra Ki-67 counting algorithm (Sectra, Linköping, Sweden)

Table 2. The primary antibodies used in this study

Antibody	Dilution	Antigen retrieval	Clone	Source
L1CAM	1:10,000	Ventana CC1 at 100ºC	UJ127 (monoclonal)	Millipore, Temecula, USA
NFkB p65/RELA	1:1,000	Ventana CC1 at 100ºC	D14E12 (monoclonal)	Cell Signaling, Boston, USA
YAP1	1:300	Ventana CC1 at 100ºC	SC-101199 (monoclonal)	Santa Cruz, Texas, USA
H3K27me3	1:100	Ventana CC1 at 100ºC	C36B11 (monoclonal)	Cell Signaling, Boston, USA
EZHIP (CXorf67)	1:300	Ventana CC1 at 100ºC	HPA004003 (polyclonal)	Millipore, Temecula, USA
GFAP	1:200	Ventana CC1 at 100ºC	6F2 (monoclonal)	DAKO, Glostrup, Denmark
K27M	1:1,000	Ventana CC1 at 100ºC	ABE419 (polyclonal)	Milipore, Temecula, USA
Ki67	1:100	Ventana CC1 at 100ºC	M7240 (monoclonal)	DAKO, Glostrup, Denmark
P16	1:100	Ventana CC1 at 100ºC	E6H4 (monoclonal)	Ventana, Export, USA
P53	1:1000	Ventana CC1 at 100ºC	DO7 (monoclonal)	DAKO, Glostrup, Denmark
pHH3	1:100	Ventana CC1 at 100ºC	369A-15 (polyclonal)	Cell Marque, Rocklin, USA

:, GFAP, glial fibrillary acidic protein; K27M, antibody for Histon Lys27Met; pHH3, phosphorylated Histone H3

DNA and RNA extraction and genetic studies

Representative areas of the tumour with >90% tumour cell content were outlined on the FFPE sections for macrodissection. DNA and RNA extractions were performed from serial sections using the Maxwell® RSC DNA FFPE Kit (Promega, Madison, WI), according to the manufacturer's instructions.

NGS was performed in 60 cases of EPNs (16 ST-, 23 PF-, and 21 SP-EPNs) with the NextSeq™ 550 system (Illumina, San Diego, CA) using a customized brain tumour gene panel (FIRST Brain Tumour Panel of SNUH), which contains 212 genes including *MYCN*, and 54 fusion genes including *ZFTA, RELA*, and *YAP1*. This gene panel is a combined DNA and RNA panel that was approved by the Korean Ministry of Food and Drug Safety.

Sequencing data were analysed using the SNUH FIRST Brain Tumour Panel Analysis pipeline. We performed quality control of the FastQ file and analyzed only the data that met the criteria. Paired-end alignment to the hg19 reference genome was performed using BWA-mem and GATK Best Practice [37]. After this step, an "analysis-ready BAM" was produced. To determine if further variant calling was appropriate, second quality control was performed. In the pipeline, Single nucleotide variants (SNVs), insertions/deletions (indels), copy number variations (CNVs), and translocations were analysed using more than two analysis tools, including in-house and open-source software. The open-source tools used were GATK UnifedGenotyper, SNVer, and LoFreq for SNV/InDel detection [38], Delly and Manta for translocation

discovery [39], THetA2 for purity estimation, and CNVKit for CNV calling [40-43]. SnpEf annotated the variants detected from various databases, such as RefSeq, COSMIC, dbSNP, ClinVar, OncoKB, and gnomAD. The germline variant was then filtered using the population frequency of these databases (>1% population frequency). Finally, the variants were confirmed through a comprehensive review of a multidisciplinary molecular tumour board. Whole exome sequencing was carried out in 5 cases of EPNs, which were evaluated with similar pipelines of NGS using brain tumor-targeted gene panel.

Meta-analysis To verify the prognostic effect of the Ki-67 labeling index, 11 articles published between 2000 and 2021 were reviewed [16, 18, 26–34]. Ki-67 cut-off, OS, PFS, HR, 95% CI, and P-value were included in the meta-analysis. In multiple studies, where cohorts overlapped, the most complete was used. Cochran's Q test was applied to determine statistical interstudy heterogeneity: Q >40 and P-value>0.10 (not 0.05) were considered to determine the presence of inter-study heterogeneity [44].

Statistical analysis

The survival rate of patients according to clinical, pathological, and genetic factors was analyzed using Kaplan–Meier survival analysis and log-rank test. Cox regression analysis was used in univariate and multivariate analysis to study the prognostic impacts of clinical and histopathological parameters. First, the influence of each variable was evaluated, and $P \leq 0.05$ was interpreted as statistical significance. Second,

the prognostic effect and independence were evaluated by examining only the variables with P≤0.05 in the multivariate analysis. All statistical analyses were performed using SPSS 25 (IBM, Armonk, NY), R version 3.5.3 (R Foundation, Vienna, Austria), and survminer 0.4.6 packages.

RESULTS

Epidemiology and subgroup of ST-, PF- and SP-EPN

IHC and molecular studies successfully reclassified 141 primary EPNs, including 17 (12%) ST-EPNs, 58 (41%) PF-EPNs, and 66 (47%) SP-EPNs (Fig. 1, Table 1). ST-EPNs-ZFTA and ST-EPN-YAP1 were 94% and 6% out of 17 ST-EPNs. The frontal lobe was the most commonly affected area. The median age of 16 ST-EPN-ZFTA patients was 14 years (range 1–51 years, 44%: younger than 10 years). All were ZFTA-RELA fusion except for one ZFTA-MAML2 fusion. PFA and PFB consisted of 71% and 29% of 58 PF-EPNs. Overall, 70% of all PF-EPNs and 98% (40/41) of PFA-EPNs occurred in children (median 3 years, range 1–16 years). One clear-cell PFA-EPN occurred in a 38-year-old woman. One hundred percent of PFB-EPNs occurred in adults (median age 41 years, range 21–69 years). The fourth ventricle was the most commonly affected site. Most patients with PFA-EPNs received adjuvant treatments after surgical resection. The t-SNE clustering with EPIC 850K methylation was performed in four PFB-EPNs, to confirm the molecular subtypes, which included

three exceptional tumors with high Ki-67 labeling indices (8.4%, 12.8% and 24.8%) and one conventional case with low Ki-67 labeling index (4.8%). The t-SNE clustering revealed clear subtypes regardless of the histological grades. In addition, four PFB-EPNs was clustered with previously known PFB group by t-SNE clustering regardless of the histological grades (Fig 7). Here, we clarify, in our results “grade 2” and “grade 3” are defined as “Ki67<7%” and “Ki67≥7%” according to our proposal on histological grading. In 66 cases of SP-EPNs, grade 2 and grade 3 were 92% and 8%, respectively and 89% were adults and 11% were children. Grade 3 SP-EPNs occurred in young patients (median 26 years; range 5–49 years, child: adult=4: 6), whereas grade 2 EPNs occurred in a broad age range of patients (median 49 years; range 8–73 years). The cervical spinal cord was the most frequently affected site by grade 2 SP-EPNs (74%, 45/61). NF2 alterations were observed in 79% (16/21) of SP-EPNs that had undergone NGS, with exception of three known NF2 patients. Three NF2 patients presented with multiple benign tumors, including meningiomas or schwannomas in addition to WHO grade 2 EPN. Our cohort did not have MYCN amplified SP-EPNs. NF2 copy number aberration was found in 81.5% (13/16) of NGS performed WHO grade 2 SP-EPNs (NF2 deletion in 44%; monosomy 22 in 37.5%). The remaining three cases each had multiple CNVs, monosomy 6, and a balanced chromosome without mutation. NF2 alteration was found in 60% (3/5) of WHO grade 3 SP-EPNs; two pathogenic mutations of NF2 (splicing, c.1122+1G>A, and splicing, c.599+1G>A), and one NF2 gene deletion. The remained one had

ZFTA-YAP1 fusion, which was just reported. The other one had a balanced chromosome with no mutations. Thus, NF2 status was not related to histological grade or biological behavior.

The results of the immunohistochemical study

L1CAM was positive in 94% (16/17) of ST-EPNs, which had *ZFTA-RELA* fusion (15 cases) and *ZFTA-MAML2* (1 case) by NGS. One case (6%) of ST-EPN-*YAP1-MAMLD1* fusion was negative for L1CAM. All PFB-EPNs were negative for both H3K27me3 and EZHIP (Fig. 2 and table 3). There was no case of immunoreactive for K27M (antibody for histone Lys27Met). The exceptional EZHIP-negative PFA-EPN, which was reconfirmed as EPN by electron microscopy, showed characteristic ependymal features such as intracytoplasmic and intercellular microrosettes with microvilli and cilia as well as zonula adherens, but methylation study could not be performed due to poor DNA quality. It was WHO grade 3 occurred in the fourth ventricle of an adult (38-year-old).

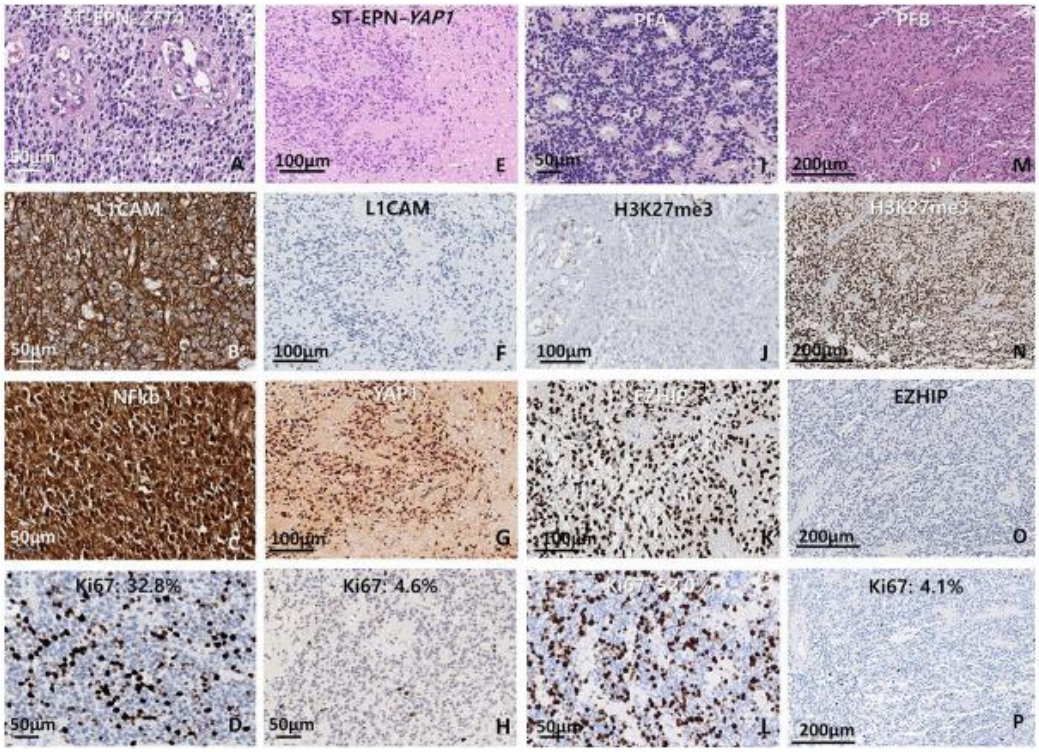

Fig. 2 Immunohistochemistry results of the ST-EPNs (A–H) and PF-EPNs (I–P). ST-EPN-ZFTA presented prominent microvascular proliferation. IHC results show robust and diffuse cytoplasmic and membranous staining for L1CAM and nuclear staining for NFkB with a high Ki-67 index (32.8%) (A–D). ST-EPN-YAP1 presented focal necrosis without microvascular proliferation. IHC results present negativity for L1CAM and strong nucleus staining of YAP1. with low Ki-67 index (4.6%) (E–H). PFA is characterized by loss of H3K27me3 expression, EZHIP overexpression, and a high level of the Ki-67 index. Some cases show extremely high proliferative activity with over 50% of the Ki-67 index (I–L). PFB is characterized by retained expression of H3K27me3, EZHIP negativity, and low Ki-67 indices (M–P). (Length of the bar, magnificence: 50 μm,×200 (A–D, H, I, L); 100 μm,×100 (E–G, J, K); 200 μm,×80) (M–P)

Table 3. Pathological, immunohistochemical and genetic features of ST-, PF- and SP-EPNs.

Parameters / Subtype	ST-EPN-*ZFTA* (n=16)	ST-EPN-*YAP1* (n=1)	IHC results	PFA (n=41)	PFB (n=17)	Genetic alteration	SP-EPN Grade 2 (n=61)	SP-EPN Grade 3 (n=5)
Conventional	16	1		38	14		49	5
papillary	-	-		2	3		2	-
clear cell	-	-		1	-		1	-
tanycytic	-	-		-	-		9	-
Microvascular proliferation	16	-		25	1		0	5
Mitoses/10 HPF: median (range)	9.5 (3-35)	1		23 (2-85)	2 (0-45)		1 (0-4)	10 (7-30)
Necrosis	13	1		30	7		7	3
Calcification	9	1		25	4		11	1
L1CAM positive	16	-	H3K27me3 loss	41	0			
NFkB positive	14	-	EZHIP overexpression	40	0			
YAP1 positive	10	1	K27M positive	0	0			
Ki-67: Median (range)	35.8% (9.0~87.4)	4.6%		31% (2.5~77.1)	3.2% (0.9~26.6)		1.7% (0.1~6.2)	30% (19~58.6)
Grade 2	0	1		3	13			
Grade 3	16	-		38	4			
ZFTA-RELA	15	-				*NF2* alteration	13	3
ZFTA-MAML2	1	-				*ZFTA-YAP1*	-	1
YAP1-MAMLD1	0	1						

Mitotic rates and Ki-67 labeling indices

There was an overlap of mitotic rates between the grade and genetic and epigenetic groups (Fig. 3A–C). In contrast, there was no overlap of the Ki-67 labeling indices between Ki-67 low- and high-groups. The Ki-67 labeling index of grade 2 and grade 3 ST-EPN ranged 1.62–4.60% (median 3.1%) and 10.4–87.4% (median 35.7%), respectively. In PF-EPNs, the median labelling index of low and high Ki-67 group was 2.8% (range 0.94–6.20%, n =16) and 30.4% (range 8.4–77.1%, n=42). We concluded that a Ki-67 index of 7% is a good cut-off for the EPN grades and in all anatomical locations (Fig. 3D–F).

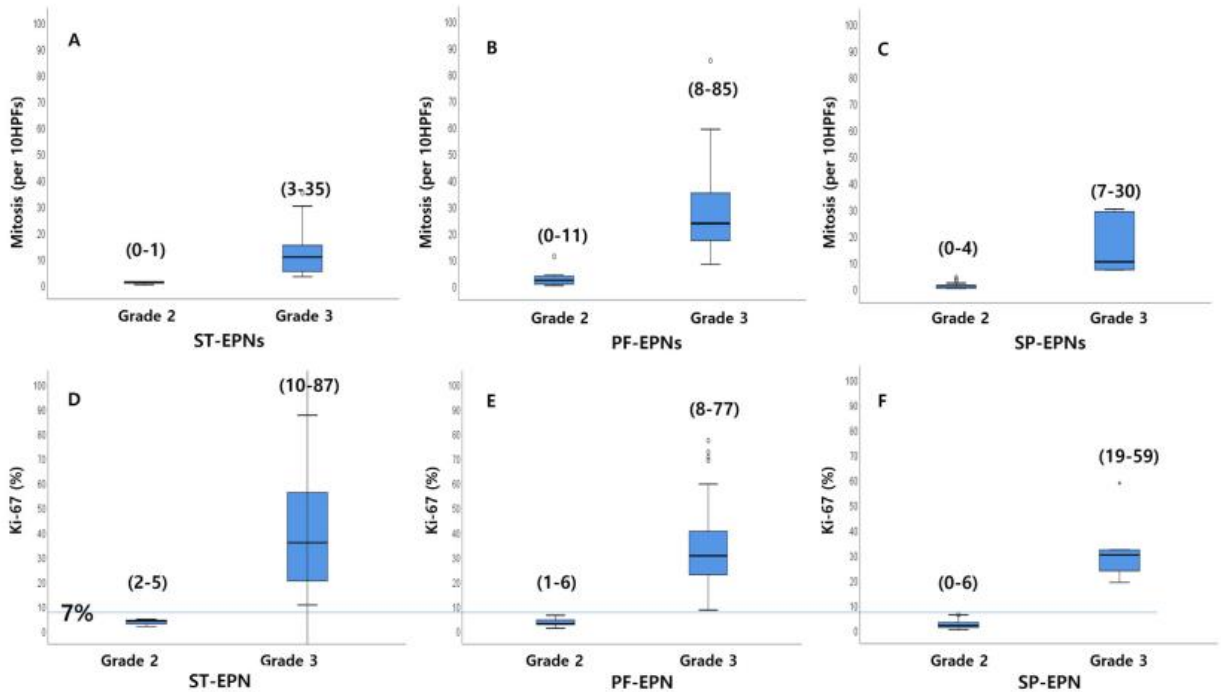

Fig. 3 The distribution of the mitotic counts (A–C) and the Ki-67 level (D–F) of ST-, PF- and SP-EPNs are plotted. There was an overlap of mitotic rates between the grades and genetic and epigenetic groups. In contrast, there was no overlap of the Ki-67 labelling indices between the Ki-67 low- and high-groups.

ZFTA fusion is not exclusively supratentorial region

One SP-EPN had a *ZFTA-YAP1* fusion identified by NGS. It presented as a 4.9 cm intramedullary lesion involving the T9-12 level of a 5 year-old boy with suspicious leptomeningeal seeding on the magnetic resonance images, and had high-grade histological features, including high cellularity, MVP, necrosis, and high proliferative activity. The tumour showed diffuse and robust cytoplasmic and membranous staining for L1CAM and nuclear staining for YAP1. The Ki-67 index was 31.6%, but it recurred 8 months after surgery. T-SNE clustering with EPIC 850K methylation array chip study showed clustering with ST-EPN-*RELA* (Fig. 4-7). This suggests that *ZFTA* fusion is not exclusive to the supratentorial region. It was similar to ST-EPN-*ZFTA* in terms of young age, high Ki-67 index, positivity for L1CAM IHC, and poor outcome.

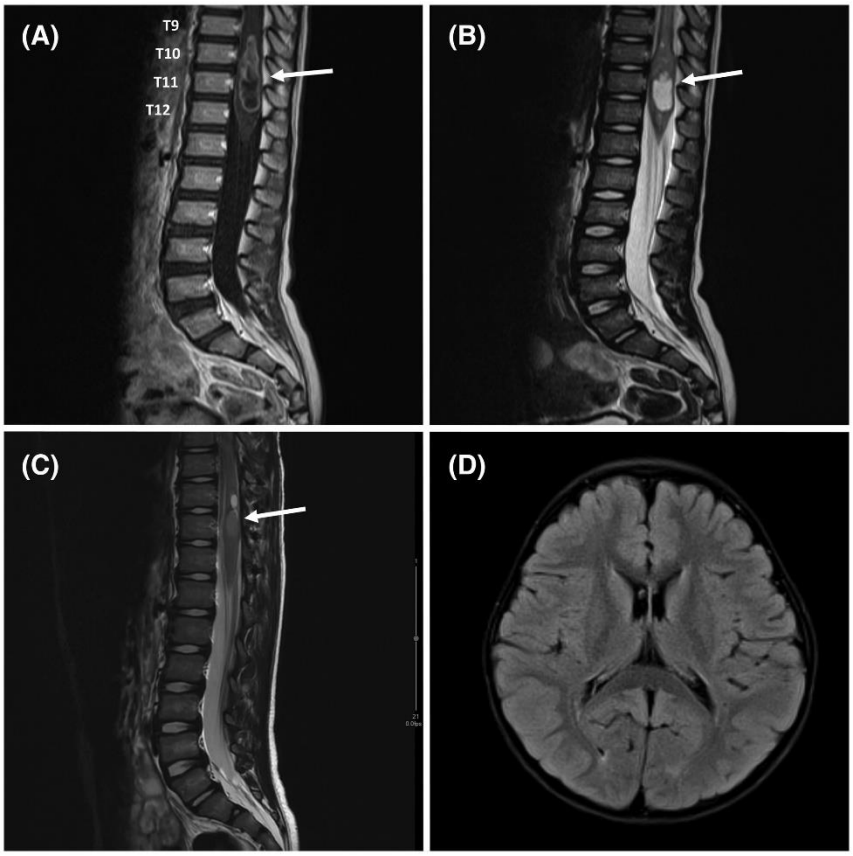

Fig. 4 MRI findings of spinal EPN–*ZFTA*-*YAP1* fusion. (A) Sagittal contrast-enhanced T1WI shows a centrally located tumor (arrow) with well-defined avid enhancing margin and central cystic or necrotic portion, which has prominent proximal spinal cord edema. Slightly prominent enhancement along with the distal spinal cord surface was also identified, which is suspicious for the leptomeningeal seeding. (B) Sagittal T2WI shows a solid and cystic lesion (arrow) involving the spinal cord at the level of T9–T12. The radiological impression was EPN versus astrocytoma. (C) The recurrent tumor was a 1.4 cm hyperintense intramedullary lesion (arrow) at the T11 level of the spinal cord on sagittal T2WI. (D) Axial T2 FLAIR image of the brain shows no remarkable lesions.

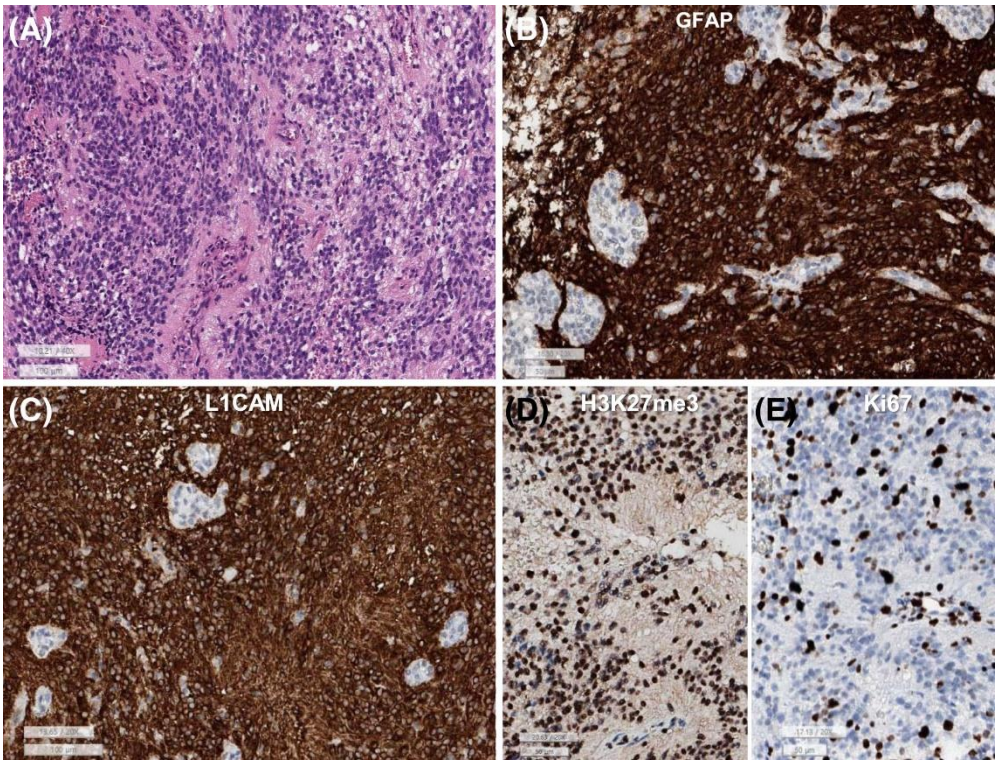

Fig. 5 Histological features of the SP-EPN-ZFTA-YPA1 (A) This spinal EPN–*ZFTA-YAP1* fusion is composed of sheets of monotonous small round to oval cells with perivascular pseudorosettes and microvascular proliferation. (B) GFAP is diffusely positive in the tumor cells except for endothelial cells of the glomeruloid microvascular proliferation. (C) L1CAM is robust positive in the cytoplasm and membrane of tumor cells. (D) H3K27me3 shows retained expression. (E) Ki-67 labeling index is high (32.4%) (A: H&E, B: GFAP, C: L1CAM, D: H3K27me3, E: Ki-67, lower bar sizes: A and C: 100 μm, B, D, and E: 50 μm)

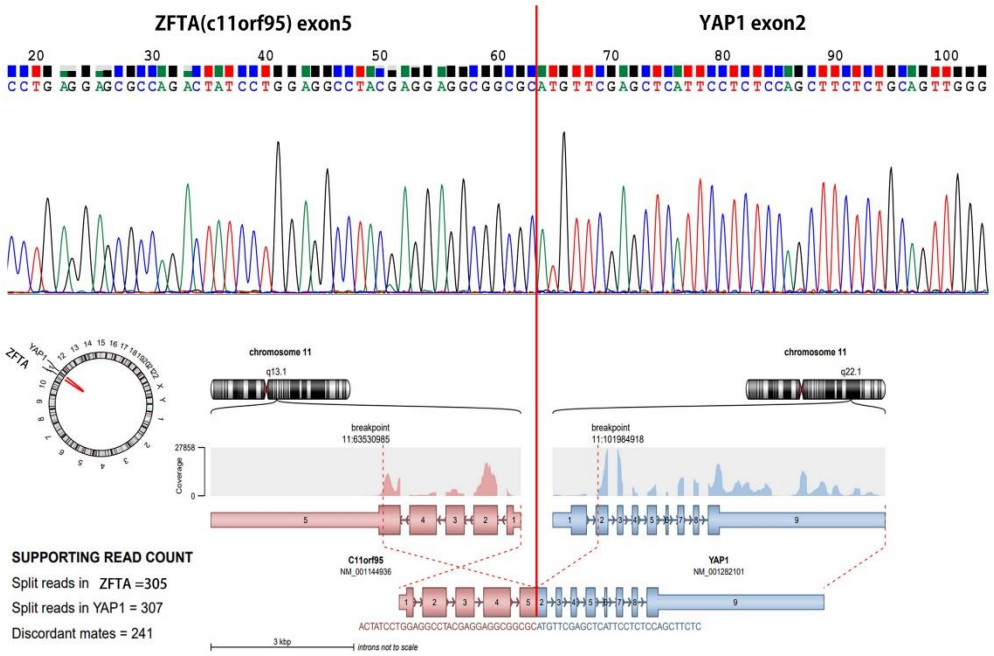

Fig. 6 *ZFTA-YAP1* fusion was confirmed by Sanger sequencing using primer set (forward: TCAAGGTGAGCACCATCAAG, backward: GATGCTGAGCTGTGGGTGTA) (upper figure). RNA was extracted from the tumor and converted to complementary DNA (c-DNA) via reverse transcription-polymerase chain reaction. *ZFTA-YAP1* RNA fusion plot (lower figure) obtained from the recurrent EPN of this patient by NGS study with FiRST brain tumor gene panel

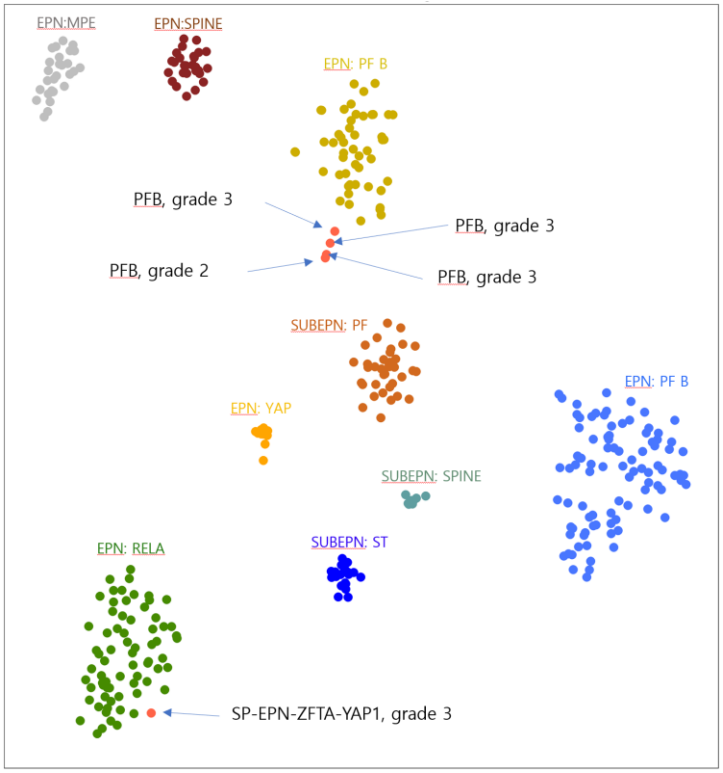

Fig. 7 Unsupervised t-SNE analysis with an overlay on the known ependymal tumor clusters from DKFZ data shows our SP-EPN–ZFTA (SNUH: presenting case) is belong to the clusters of ST-EPN–ZFTA fusion-positive, but apart from the clusters of the SP-EPN. In addition, four PFB-EPNs was clustered with previously known PFB group by t-SNE clustering regardless of the histological grades. MPE, myxopapillary EPN; PFA-EPN, posterior fossa group A EPN; PFB-EPN, posterior fossa group B EPN; PF-SUBEPN, posterior fossa-subependymoma; PN, ependymoma; SP-EPN, spinal-ependymoma; SP-SUBEPN, spinal subependymoma; ST-EPN-ZFTA, supratentorial-ependymoma ZFTA fusion-positive; ST-SUBEPN, supratentorial subependymoma; YAP1-EPN, ST-ependymoma YAP1-positive

Copy number variation in 60 ependymomas

CNV analysis by NGS was performed (16 ST-EPNs, 23 PF-EPNs, and 21 SP-EPNs) (Table 4). Of the six tumors with chromosome 9p21 deletion, 84% (5/6) recurred at least twice, four tumors (67%) had extracranial metastasis, and three patients (50%) died. Seven tumors with a 1q25 gain recurred in 87.5% (7/8); four patients (50%) had two or more recurrences, of which one patient (12.5%) had extracranial metastasis, and 2 patients (25%) died. Monosomy 6 was found in one case of ST-EPN-ZFTA, two PFA, and one PFB. One PFA-EPN with monosomy 6 had multiple recurrences and extracranial metastasis. Monosomy 11 was only observed in ST-EPN-ZFTA and there was no recurrence during the 3-year follow-up period. Chromosome 1p loss was observed in one ST-EPN-ZFTA, which also presented extracranial metastasis. A balanced chromosomal profile (n=12) was observed at all anatomical locations, including five ST-EPN-ZFTAs, one YAP1-MAMLD1 fusion-positive ST-EPN, three PFA-EPNs, and three SP-EPNs. Among them, two cases showed intracranial recurrent EPN (2/9, 22%) and one case showed extracranial metastasis. Interestingly, an SP-EPN with a balanced copy number and ZFTA-YAP1 fusion recurred 8 months after GTR which was clustered with ZFTA-RELA fusion-positive ST-EPN by the methylation profile. Multiple CNV was observed in two PFB-EPNs with no recurrence.

Table 4. Copy number variations observed in 60 NGS-performed EPNs

	ST-EPNs (n=16)		PF-EPNs (n=23)		SP-EPNs (n=21)	
	Grade 2 (n=1)	Grade 3 (n=15)	Grade 2 (n=4)	Grade 3 (n=19)	Grade 2 (n=16)	Grade 3 (n=5)
1q25 gain	-	3	-	5	-	-
Chr 11 monosomy	-	1	-	-	-	-
NF2 splicing mutation	-	-	-	-	-	2
Only NF2 gene deletion	-	-	1 (Homozygous)	-	7 (6 hemizygous, 1 homozygous)	1 (hemizygous)
Chr 22 monosomy	-	2	-	2*	6	-
Chr 6 monosomy	-	1	1	2*	1	-
CDKN2A/2B deletion	-	2 (Homozygous)	-	2 (Homozygous) 2 (Hemizygous)	-	-
Others	-	1 (1p deletion)	2 (Multiple CNV)	1 (Chr 10 monosomy) 1 (Chr 7 monosomy) 1 (Chr 19q gain) 1 (Chr 1 monosomy &Chr 9 monosomy)	1 (Multiple CNV)	-
Balanced	1	5	-	3	1	2

*: One PFA-EPN had both chromosomes 6 and 22 monosomy; CNV: copy number variation

Recurrence rate and survival

All patients with ST-EPN-ZFTA received adjuvant treatments after the surgical resection, except one case with gross total resection (GTR) only (Table 1). Despite adjuvant treatment, 56% (9/16) of ST-EPN-ZFTA had one or more recurrences and three of them died (3/9), 41% (7/16) had multiple recurrences, and 12.5% (2/16) recurred more than fve times. Extracranial metastases were found in 25% (4/16) of ST-EPN-ZFTA into the liver, lung, and salivary gland. The patient with ST-EPN ZFTA-MAML2 fusion-positive (5-year-old girl) had recurred 49 months after GTR+RT. ST-EPN YAP1-MAMLD1 fusion-positive (6-year-old girl) did not recur for 99 months after GTR, without adjuvant therapy. The 5-year and 10-year OS rates of ST-EPN-ZFTA were 93.8% and 81.3%, respectively. The 5-year and 10-year PFS rates of ST-EPN-ZFTA were 50.0% and 43.8%, respectively. The Kaplan–Meier analysis of PFS rates was significantly worse for PFA than for PFB (P=0.007); 71% of PFA-EPN (29/41) and 24% (4/17) of PFB-EPNs. Multiple recurrences and extracranial metastases were observed in 39% and 24%, respectively. Among them, 44% were younger than 5 years of age. The 5-year and 10-year OS rates of PFA-EPN were 73.2% and 70.7%, respectively. The 5- and 10-year PFS rates of PFA-EPN were 36.6% and 29.3%, respectively. None of the PFB-EPNs showed extracranial metastasis. Of the five grade 3 SP-EPNs, three received GTR+RT and two underwent GTR. All grade 2 patients had only GTR, except for two patients receiving STR+RT. OS and PFS were similar to the follow-up period for WHO grade 2 SP-EPNs (OS:

median 39 months; range 0–1003 months, PFS: median 38 months; range 0–1003 months).

Univariate and multivariate analysis: Ki-67 index is the only independent prognostic factor of intracranial EPNs

To study the prognostic impact of clinical and histopathological parameters on intracranial EPNs, we studied the univariate and multivariate analysis in a total of 75 intracranial EPNs. The variables considered in OS and PFS were age (age < 4 vs. age ≥4), gender, location, the extent of resection (GTR vs. STR), microvascular proliferation (MVP), necrosis, nuclear pleomorphism, mitotic index, Ki-67 labeling index and three biomarkers L1CAM, H3K27me3, and EZHIP. Only a Ki-67 index was significantly associated with OS in univariate analysis (P = 0.046) (Table 5A). The microvascular proliferation (P = 0.048), necrosis (P = 0.044), mitotic activity (P = 0.001), Ki-67 index (P < 0.001), H3K27me3 loss (P = 0.016), and EZHIP overexpression (P = 0.015) were significantly associated with PFS. Age and the extent of resection showed clear trends but did not reach statistical significance. In multivariate analysis, the Ki-67 index (P = 0.001, as continuous data) was the only independent prognostic factor associated with PFS (Table 5B-1, 5B-2). Note the increased hazard ratio when Ki-67 index was applied as categorical data (index ≥ 7% vs. < 7%) in both OS (HR=7.6, Table 5A) and PFS (HR=4.4, Table 5B-2).

Table 5. Univariate and multivariate analysis of clinicopathological parameters on OS and PFS in a total of 75 intracranial EPNs

(A) Overall survival

Variables		Univariate		
		P	HR	95%CI
Age	age ≥ 4 vs. < 4	0.219	1.72	0.72-4.11
Sex	Male vs. Female	0.36	0.66	0.27-1.61
Location	ST vs. PF	0.97	1.02	0.36-2.87
Extent of resection	GTR vs. STR	0.99	1.003	0.41-2.44
Histologic type	classic vs. anaplastic	0.38	0.67	0.27-1.65
Microvascular proliferation	Present vs. absent	0.79	0.89	0.37-2.11
Necrosis	Present vs. absent	0.15	0.45	0.15-1.34
Nuclear pleomorphism	Present vs. absent	0.39	0.62	0.21-1.83
Mitotic index	Continuous data	0.051	1.02	1.00-1.05
Ki-67(a)	Continuous data	0.046	1.02	1.00-1.04
Ki-67(b)	index ≥ 7% vs. < 7%	0.048	7.631	1.01-57.43
L1CAM expression	Positive vs. negative	0.94	1.05	0.30-3.70
H3K27me3 loss	Loss vs. retained expression	0.06	6.86	0.91-51.94
EZHIP overexpression	Overexpression vs. negative	0.11	0.40	0.13-1.23

(Ki-67 labeling index was applied as continuous data(a) and categorical data(b).)

(B-1) Progression-free survival

Variables		Univariate			Multivariate		
		P	HR	95%CI	P	HR	95%CI
Age	age ≥ 4 vs. < 4	0.055	0.95	0.89-1.001			
Sex	Male vs. Female	0.51	0.81	0.45-1.48			
Location	ST vs. PF	0.89	1.04	0.55-1.99			
Extent of resection	GTR vs. STR	0.07	0.58	0.33-1.05			
Histologic type	classic vs. anaplastic	0.13	0.63	0.35-1.15			
Microvascular proliferation	Present vs. absent	0.048	0.55	0.30-0.99	0.69	1.16	0.56-2.40
Necrosis	Present vs. absent	0.044	0.5	0.25-0.98	0.10	0.53	0.25-1.12
Nuclear pleomorphism	Present vs. absent	0.19	0.62	0.30-1.26			
Mitotic index	Continuous data	0.001	1.03	1.010-1.040	0.36	0.99	0.95-1.02
Ki-67	Continuous data	<0.001	1.03	1.015-1.041	0.001	1.03	1.01-1.04
L1CAM expression	Positive vs. negative	0.62	0.83	0.39-1.75			
H3K27me3 loss	Loss vs. retained	0.016	2.58	1.19-5.60	0.77	1.19	0.37-3.80
EZHIP overexpression	Overexpression vs. negative	0.015	0.44	0.23-0.85	0.06	0.53	0.27-1.03

(Ki-67 labeling index was applied as continuous data)

(B-2) Progression-free survival

Variables		Univariate			Multivariate		
		P	HR	95%CI	P	HR	95%CI
Age	age ≥ 4 vs. < 4	0.055	0.95	0.89-1.001			
Sex	Male vs. Female	0.51	0.81	0.45-1.48			
Location	ST vs. PF	0.89	1.04	0.55-1.99			
Extent of resection	GTR vs. STR	0.07	0.58	0.33-1.05			
Histologic type	classic vs. anaplastic	0.13	0.63	0.35-1.15			
Microvascular proliferation	Present vs. absent	0.048	0.55	0.30-0.99	0.57	0.81	0.39-1.68
Necrosis	Present vs. absent	0.044	0.5	0.25-0.98	0.16	1.74	0.81-3.77
Nuclear pleomorphism	Present vs. absent	0.19	0.62	0.30-1.26			
Mitotic index	Continuous data	0.001	1.03	1.010-1.040	0.61	1.01	0.98-1.03
Ki-67	index ≥ 7% vs. < 7%	0.002	5.10	1.80-14.50	0.007	4.36	1.51-12.63
L1CAM expression	Positive vs. negative	0.62	0.83	0.39-1.75			
H3K27me3 loss	Loss vs. retained	0.016	2.58	1.19-5.60	0.55	0.70	0.22-2.28
EZHIP overexpression	Overexpression vs. negative	0.015	0.44	0.23-0.85	0.10	1.78	0.91-3.50

(Ki-67 labeling index was applied as categorical data)

The result of meta-analysis for identifying the prognostic effect of Ki-67

A further meta-analysis of 11 publications [45-55], to identify the significance of Ki-67 labeling indices with the OS, showed that the overall HR was 3.95 (95% CI 2.59–6.03, P<0.0001) indicating that increased levels of Ki-67 were associated with worse outcomes. The inter-study heterogeneity was negligible (Q=22.8; P=0.01) (Fig. 8A) The overall HR of PFS of the five eligible studies was 6.25 (95% CI 3.42–11.42, P<0.0001), suggesting a high association between increased Ki-67 indices and poor prognosis (Q=7.41; P=0.11) (Fig. 8B)

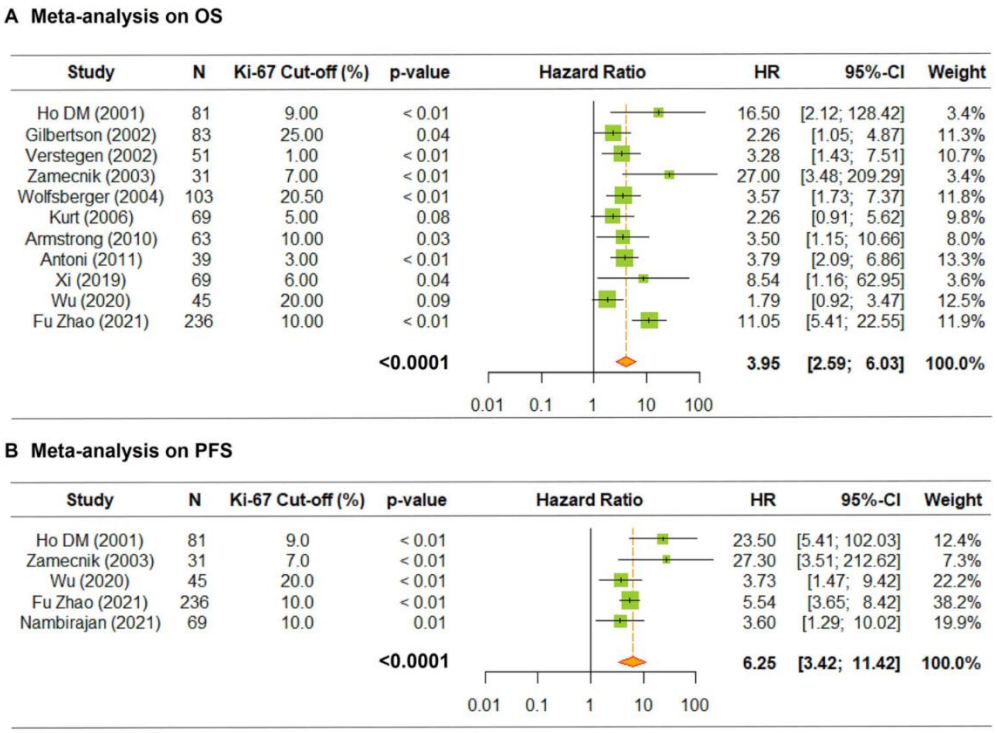

Fig. 8 Meta-analysis about the prognostic value of Ki-67 index on OS (**A**) and PFS (**B**) of intracranial EPNs. Increased levels of Ki-67 were associated with poor survival rates (both $P < 0.0001$). The overall values were written in bold.

Kaplan Meier survival analysis according to Ki-67 labeling indices, H3K27me3 loss, and EZHIP overexpression

The Kaplan–Meier survival analysis according to grade, the prognosis was worse in grade 3 than grade 2, but did not reach the statistical significance in ST-, and SP-EPNs (Fig. 9A, B and 9E, F) because the limitation of the number of WHO grade 2 ST-EPNs (6%) and WHO grade 3 SP-EPNs (8%). Both OS and PFS of PF-EPNs were strongly associated with the grades based on 7% Ki-67 (P=0.021 and 0.001, respectively) (Fig. 9C, D). Loss of H3K27me3 (P=0.007) and overexpression of EZHIP (P=0.002) were significantly associated with a poor prognosis. H3K27me3 and EZHIP were statistically significantly associated by Fisher's exact test (P<0.0001) (Fig. 10)

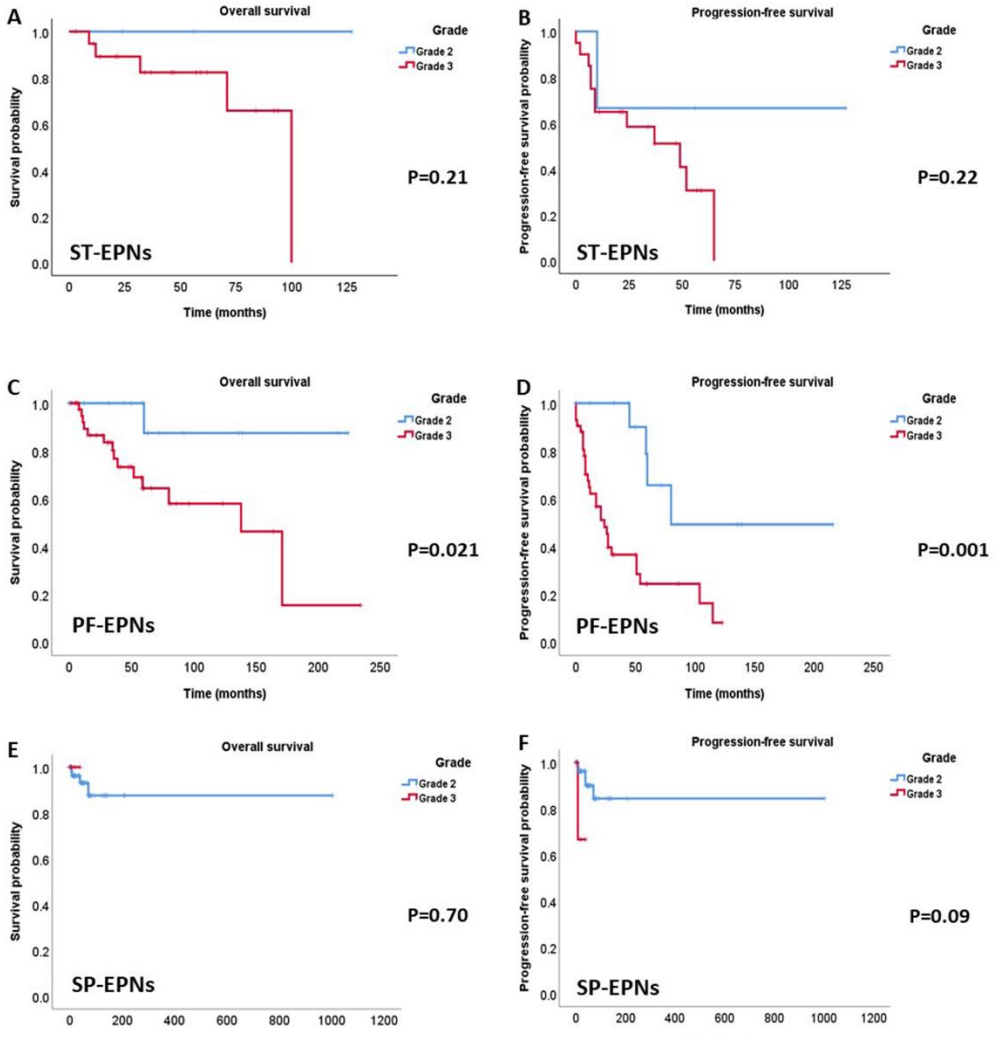

Fig. 9 Kaplan–Meier survival analysis according to the grades in ST-, PF- and SP-EPNs. Grade 2 and grade 3 were designated by 7% of the Ki-67 cut-off. Grade 3 shows a significantly worse prognosis than grade 2, both in OS and PFS in PF-EPNs (C, D). However, the survival difference of ST- and SP-EPNs by the grade did not reach statistical significance (A, B and E, F)

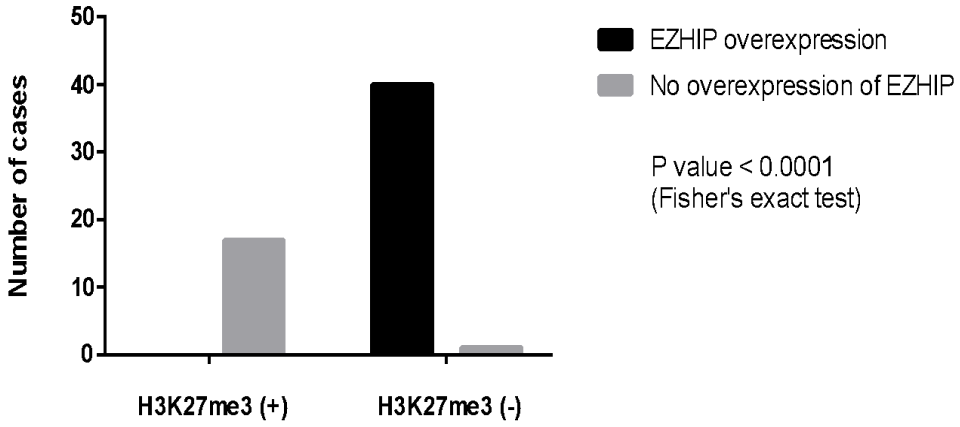

Fig. 10 H3K27me3 and EZHIP were statistically significantly associated by Fisher's exact test (P<0.0001) and diagnostic in PF-EPNs.

A precise and easily applicable schematic diagnostic flow in clinical practice

In our study, L1CAM and H3K27me3 (and/or EZHIP) IHC and Ki67 labeling indices were sufficient to classify intracranial EPNs, which could be both practical and cost-effective. H3K27me3 loss should be considered before EZHIP because the global reduction of H3K27me3 is the main mechanism of PFA-EPNs. For SP-EPNs, most had NF2 gene deletion, monosomy 22, or rarely an NF2 genesplicing mutation but these genetic changes did not affect the patient's outcomes. The Ki-67 index was shown to be a powerful prognostic factor in multivariate analysis, and a lower than 7% cutoff was a good indicator for grades 2 EPNs. We proposed a schematic diagnostic flow of EPNs, which can be a useful, accurate, and cost-effective diagnosis in clinical and pathological practice (Fig. 11).

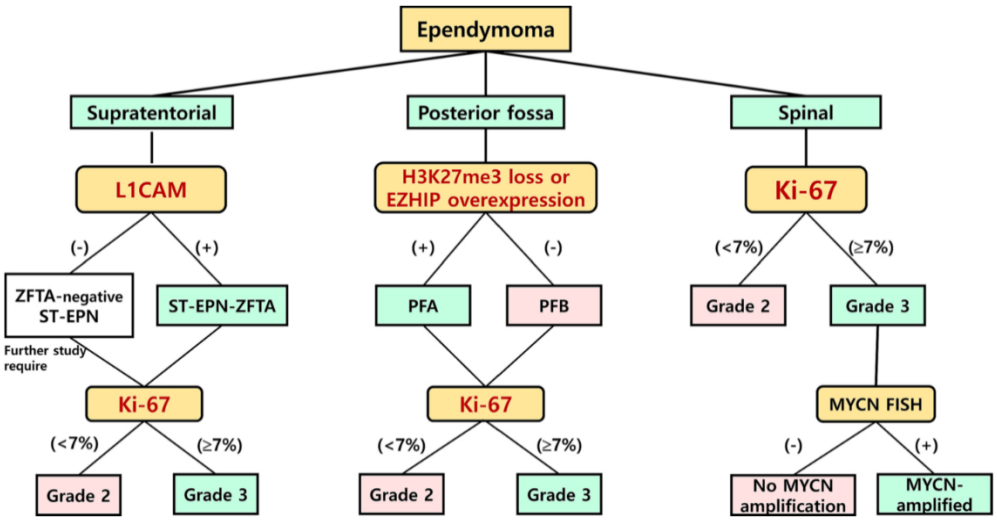

Fig. 11 A schematic diagnostic flow that we propose. EPNs should be classified by the anatomic locations and the surrogate markers reflecting their genetic or epigenetic alteration. ST-EPNs can be subdivided according to L1CAM-IHC. All L1CAM-positive EPNs can be considered as ZFTA fusion-positive EPNs. ZFTA-negative-ST-EPNs are heterogeneous tumors, which can be divided as WHO grade 2 or 3 according to the Ki-67 labeling index. PF-EPNs are subdivided according to H3K27me3 and EZHIP status. Both PFA and PFB can have both WHO grade 2 and 3 according to Ki-67 labeling indices. A Ki-67 index of 7% or more should be considered WHO grade 3. MYCN-FISH is not needed in WHO grade 2 SP-EPNs but essential in WHO grade 3 SP-EPNs.

DISCUSSION

Reclassified our 144 EPNs by molecular subtyping

We successfully reclassified our 144 EPNs by cIMPACT-NOW update 7 using four biomarkers of L1CAM, H3K27me3, EZHIP, and Ki-67. Reclassified ependymomas showed a high correlation with pathological grade, patients' age, and biological behavior. Interestingly, Kaplan-Meier survival analysis and multivariate analysis showed that risk stratification by molecular subgrouping was superior to histological grading [6]. We learned that 70% of ST-EPN-*ZFTA* and almost all PFA-EPN occurred in children, but almost all PFB occurred in adults. 92% of low-grade SP-EPN were adults. Fusion genes were found in ST-EPN, with one exception. The *ZFTA-YAP1* fusion was found in high-grade SP-EPN. L1CAM was a practically excellent surrogate marker in predicting *ZFTA*-fusion, and H3K27me3 loss and EZHIP overexpression were excellent biomarkers to identify PFA-EPN. In SP-EPNs, *NF2* mutation or deletion was the underlying genetics, but it did not affect biological behavior. 1q25 gain, monosomy 6, and CDKN2A/2B homozygous deletion were related to poor outcomes including multiple recurrences and extracranial metastases, which was similar to previous reports [13, 56]. Reclassification of EPNs by molecular subtyping is superior to classifying by histology only.

Prognostic impacts of various parameters

The prognostic and predictive effects of histological parameters of EPN, including

histological grade, are known to be controversial. According to Figarella-Branger et al., STR, loss of histological differentiation, high Ki-67 index (≥1%), and age younger than 4 were associated with inferior PFS [57]. In one multivariate analysis by Horn et al., age (age<3 vs. age≥3), histologic grade (grade 2 vs. grade 3), and extent of resection affected OS and PFS [58].

In our study, 56% of ST-EPN-*ZFTA* recurred repeatedly despite GTR plus RT and three of them (19%) died. In this reason, the extent of resection doesn't fully work for a prognostic factor and we need an additional factor, although maximal resection is a very important treatment option. In our study, the multivariate analysis showed that Ki-67 was the only independent prognostic factor in both PFS and OS, which can be supported by previous reports. Malgulwar et al.'s study revealed that L1CAM positivity and high Ki-67 labeling indices were associated with poor PFS, but the age and the degree of resection did not show significance to survival [16].

The extent of resection and age also had prognostic impact, though they did not reach the statistical significance in our study. Through our study, we emphasize that Ki-67 labeling index is a good biomarker to predict the prognosis and decide the post-operative management.

The cutoff of the Ki-67 labeling index

In our study, the Ki-67 index (cut-off of 7%) was well correlated with the WHO grades and PFS of our series of EPNs in all anatomical locations. However, our cohort

of EPNs did not show statistical significance in OS because our cohort has limitations in patients' number and follow-up period. In addition, the patients in our cohort survived longer, the 5-year survival rates of higher grade (WHO grade 3) EPNs were 93.8%, 73.2%, and 93.8% in ST-EPN-*ZFTA*, PFA, and SP-EPN-*NF2*, respectively, and the 10-year survival rates were 81.3%, 70.7%, and 87.5%, respectively, suggesting that EPNs are chronic diseases, despite multiple local recurrence and distant metastases.

Exceptionally graded cases and Ki-67 as the additional objective parameter in grades and prognosis

Although genetic and epigenetic subtypes were highly associated with the prognosis in intracranial EPNs, the previous studies reported that they do not necessarily determine the grades because there are some exceptional cases, such as grade 2 PFA with good prognosis, and grade 3 PFB and ST-EPN-*YAP1* with poor outcomes [10, 59].

Reproducible cut-offs for Ki-67 labeling indices have been proposed in astrocytic and oligodendroglial tumors to predict the outcomes [60-63]. Similarly, our meta-analysis with 11 published papers showed that increased Ki-67 labeling indices were strongly correlated with poor OS and PFS of EPNs (both $P<0.0001$).

Significant heterogeneity of staining techniques, such as different antibody clones, dilution, and counting methods may affect cut-off. However, we used the same

thickness of tissue sections and the same immunostaining method, and AperioSpectrum plus image analyzer to count all cases to maintain the same conditions and to minimize the inter-observer variability.

In our study, we found area-to-area differences of Ki-67 labeling indices, and grading based on the 7% cut-off showed a strong association with genetic subtypes of EPNs and clinical outcomes. We suggest that a Ki-67 index of 7% is the most reliable cut-off for grading in all anatomical locations. Our cut-off is also supported by the study of Zamecnik et al. in which a Ki-67 labeling index more than and equal to 7% was associated with an inferior outcome in both OS and PFS of EPN. The 7% cutoff of Ki-67 labeling index is significant in several reasons: This study initially maintained the same condition in all cases including the antibody, dilution, antigen retrieval and analysis at least three hot spots; Morphometric analysis was conducted in all cases to maximize the objectivity and rule out the subjectivity, which indicated its reproducibility; Survival analysis delineated that grades by this cutoff well correlated with prognosis; Although molecular subtyping of EPNs by new WHO classification correlates with the biological behavior, there are still some exceptional cases in which molecular subtyping and biological behavior do not correlate, therefore, additional factors are needed to predict their clinical behavior more accurately. In our study, 7% cutoff of Ki-67 labeling index played a useful role in grading and predicting prognosis of EPNs.

Copy number variations and outcomes

In addition, our results showed that chromosome 1q25 gain and CDKN2A/2B loss were significant poor prognostic factors indicating a dismal prognosis, such as multiple recurrence or extracranial metastasis. The monosomy 6 and balanced chromosomal profile were the next worse prognostic factor, also indicating multiple recurrence and extracranial metastasis. However, multiple CNVs without the aforementioned CNVs were associated with favorable outcomes.

In our study, every tumor with chromosome 1q25 gain, except one, recurred at least once. Two grade 3 ST-EPN-ZFTA with homozygous deletion of CDKN2A/2B and two grade 3 PFA-EPNs with hemizygous deletion exhibited extracranial metastasis. Our results correspond with the previous report by Korshunov et al. that gain of 1q and homozygous deletion of CDKN2A were associated with unfavorable outcome. Furthermore, they suggested that 1q25 gain and CDKN2A/2B deletions were independent prognostic factors by multivariate analysis [56, 64]. On the other hand, Rajeshwari et al. presented an opposite result that gain of 1q did not show significant association with various clinicopathological parameters. Additionally, in our study, gain of 1q was observed in four children and three adults. All were older than 4-years-old except one ST-EPN-ZFTA. This finding is similar to previous studies that 1q gain is more frequently observed in older children (> 4 years old) [65, 66]. Also, 1q 25 gain was mainly observed in PFA-EPNs followed by in ST-EPN-ZFTA, similar to previous report [6]. Correlation between CDKN2A deletion and poor outcome has been studied in various CNS tumors including astrocytoma, IDH-wildtype GBM and

diffuse malignant IDH-mutant gliomas [67-69].

An exceptional SP-EPN with *ZFTA-YAP1* fusion

Our case is the first case of SP-EPN harboring a ZFTA-YAP1 fusion [70]. Unsupervised t-SNE analysis with an overlay on the known ependymal tumor clusters revealed that our case belonged to ST-EPN-RELA (now the same as *ZFTA*-fusion-positive ST-EPN), not SP-EPN. Most importantly, the DNA methylation profile and biological behavior of this case were similar to those of ST-EPN-ZFTA, despites of its location. Our case is an exceptional tumor that breaks the dogma that regards ependymoma as a significantly different tumor according to its anatomical loci. The biomechanism of *ZFTA*- fusion needs to be determined to realize the goal of targeted therapy. This goal is crucial for EPNs, which are resistant to chemotherapy with maximal surgical resection and radiation therapy as the currently available treatment options.

CONCLUSION

Here, we reclassified EPNs according to the diagnostic criteria of cIMPACT-NOW update 7 and the 2021 WHO classification. From our study, we recommend a schematic diagnostic flow using three surrogate markers (L1CAM, H3K27me3, and EZHIP) and Ki-67 (Fig. 11), which may be a precise, easy and cost-effective diagnostic scheme for the management of patients [71].

DECLARATIONS

Ethics approval and consent to participate: The institutional review board of our hospital approved this study (IRB No: 2012-034-1179) and has therefore been performed in accordance with the ethical standards set out in the 1964 Declaration of Helsinki and its subsequent amendments. As this study is a retrospective review of anonymized electronic medical records, pathology, and NGS data utilizing a brain tumor-specific somatic gene panel, informed consent was waived from our IRB under the Korean Bioethics and Safety Act.

Consent for publication: All materials had been obtained for the medical care of the patients, which were anonymized and retrospectively reviewed. No extra-human materials were obtained for this study. Under the Korean Bioethics and Safety Act, additional consent to publish was waivered.

Availability of data and material: The datasets used and/or analyzed during the current study are available from the corresponding author on reasonable request.

Competing interests: The authors do not have any conflicts of interest to declare.

Funding: It was mentioned in the acknowledgments section.

Authors' contributions: Sung-Hye Park designed and supervised the study. Ka Young Lim, Jae-Kyung Won and Sung-Hye Park reviewed histologic slides, signed all pathological reports, and collected anonymized data for qualitative analysis. Ka

Young Lim, Jin Woo Park, Jeongwan Kang, Hyunghee Kim, and Seung Hong Choi collected and analyzed clinical, radiological, and pathological data. Seung-Ki Kim, Ji Hoon Phi, and Chun-Kee Chung treated the patients and provided clinical information. Hongseok Yun analyzed the NGS data in the sequencing of the brain tumors-targeted gene panel. Ka Young Lim, Kwanghoon Lee, and Yumi Shim performed data analysis. The manuscript was written by Ka Young Lim and Sung-Hye Park. All authors have reviewed and edited the final manuscript.

Acknowledgments: This study was supported by a grant from the Korea Health Technology R&D Project through the Korea Health Industry Development Institute (KHIDI), funded by the Ministry of Health & Welfare, Republic of Korea (grant number: HI14C1277).

Reference

1. Cacciotti, C., A. Fleming, and V. Ramaswamy, *Advances in the molecular classification of pediatric brain tumors: a guide to the galaxy.* J Pathol, 2020. **251**(3): p. 249-261.
2. Del Bigio, M.R., *Ependymal cells: biology and pathology.* Acta Neuropathol, 2010. **119**(1): p. 55-73.
3. Louis, D.N., *Central Nervous System Tumors update 2016.* 2016.
4. Taylor, M.D., et al., *Radial glia cells are candidate stem cells of ependymoma.* Cancer Cell, 2005. **8**(4): p. 323-35.
5. Ellison, D.W., et al., *cIMPACT-NOW update 7: advancing the molecular classification of ependymal tumors.* Brain Pathol, 2020. **30**(5): p. 863-866.
6. Pajtler, K.W., et al., *Molecular Classification of Ependymal Tumors across All CNS Compartments, Histopathological Grades, and Age Groups.* Cancer Cell, 2015. **27**(5): p. 728-43.
7. Ellison, D.W., et al., *Histopathological grading of pediatric ependymoma: reproducibility and clinical relevance in European trial cohorts.* J Negat Results Biomed, 2011. **10**: p. 7.
8. Kupp, R., et al., *ZFTA-translocations constitute ependymoma chromatin remodeling and transcription factors.* Cancer Discov, 2021.
9. Arabzade, A., et al., *ZFTA-RELA Dictates Oncogenic Transcriptional Programs to Drive Aggressive Supratentorial Ependymoma.* Cancer Discov, 2021.
10. Andreiuolo, F., et al., *Childhood supratentorial ependymomas with YAP1-MAMLD1 fusion: an entity with characteristic clinical, radiological, cytogenetic and histopathological features.* Brain Pathol, 2019. **29**(2): p. 205-216.
11. Pietsch, T., et al., *Supratentorial ependymomas of childhood carry C11orf95-RELA fusions leading to pathological activation of the NF-kappaB signaling pathway.* Acta Neuropathol, 2014. **127**(4): p. 609-11.
12. Sasaki, A., et al., *Review of ependymomas: assessment of consensus in*

pathological diagnosis and correlations with genetic profiles and outcome. Brain Tumor Pathol, 2019. **36**(2): p. 92-101.

13. Lillard, J.C., et al., *Pediatric Supratentorial Ependymoma: Surgical, Clinical, and Molecular Analysis.* Neurosurgery, 2019. **85**(1): p. 41-49.
14. Zschernack, V., et al., *Supratentorial ependymoma in childhood: more than just RELA or YAP.* Acta Neuropathol, 2021. **141**(3): p. 455-466.
15. Parker, M., et al., *C11orf95-RELA fusions drive oncogenic NF-kappaB signalling in ependymoma.* Nature, 2014. **506**(7489): p. 451-5.
16. Malgulwar, P.B., et al., *C11orf95-RELA fusions and upregulated NF-KB signalling characterise a subset of aggressive supratentorial ependymomas that express L1CAM and nestin.* J Neurooncol, 2018. **138**(1): p. 29-39.
17. Fogel, M., et al., *L1 expression as a predictor of progression and survival in patients with uterine and ovarian carcinomas.* Lancet, 2003. **362**(9387): p. 869-75.
18. Boo, Y.J., et al., *L1 expression as a marker for poor prognosis, tumor progression, and short survival in patients with colorectal cancer.* Ann Surg Oncol, 2007. **14**(5): p. 1703-11.
19. Ben, Q.W., et al., *Positive expression of L1-CAM is associated with perineural invasion and poor outcome in pancreatic ductal adenocarcinoma.* Ann Surg Oncol, 2010. **17**(8): p. 2213-21.
20. Kiefel, H., et al., *Linking L1CAM-mediated signaling to NF-kappaB activation.* Trends Mol Med, 2011. **17**(4): p. 178-87.
21. Pajtler, K.W., et al., *YAP1 subgroup supratentorial ependymoma requires TEAD and nuclear factor I-mediated transcriptional programmes for tumorigenesis.* Nat Commun, 2019. **10**(1): p. 3914.
22. *<9. Lowered H3K27me3 and DNA hypomethylation define.pdf>.*
23. Rosenbluh, J., et al., *beta-Catenin-driven cancers require a YAP1 transcriptional complex for survival and tumorigenesis.* Cell, 2012. **151**(7): p. 1457-73.
24. Robinson, M.H., et al., *Upregulation of the chromatin remodeler HELLS is mediated by YAP1 in Sonic Hedgehog Medulloblastoma.* Sci Rep, 2019.

9(1): p. 13611.

25. Bender, S., et al., *Reduced H3K27me3 and DNA hypomethylation are major drivers of gene expression in K27M mutant pediatric high-grade gliomas.* Cancer Cell, 2013. **24**(5): p. 660-72.
26. Mack, S.C., et al., *Epigenomic alterations define lethal CIMP-positive ependymomas of infancy.* Nature, 2014. **506**(7489): p. 445-50.
27. Jain, S.U., et al., *PFA ependymoma-associated protein EZHIP inhibits PRC2 activity through a H3 K27M-like mechanism.* Nat Commun, 2019. **10**(1): p. 2146.
28. Hubner, J.M., et al., *EZHIP/CXorf67 mimics K27M mutated oncohistones and functions as an intrinsic inhibitor of PRC2 function in aggressive posterior fossa ependymoma.* Neuro Oncol, 2019. **21**(7): p. 878-889.
29. Jenseit, A., et al., *EZHIP: a new piece of the puzzle towards understanding pediatric posterior fossa ependymoma.* Acta Neuropathol, 2022. **143**(1): p. 1-13.
30. Lee, C.H., C.K. Chung, and C.H. Kim, *Genetic differences on intracranial versus spinal cord ependymal tumors: a meta-analysis of genetic researches.* Eur Spine J, 2016. **25**(12): p. 3942-3951.
31. Mendrzyk, F., et al., *Identification of gains on 1q and epidermal growth factor receptor overexpression as independent prognostic markers in intracranial ependymoma.* Clin Cancer Res, 2006. **12**(7 Pt 1): p. 2070-9.
32. Aguilera, D.G., et al., *Neurofibromatosis-2 and spinal cord ependymomas: Report of two cases and review of the literature.* Childs Nerv Syst, 2011. **27**(5): p. 757-64.
33. Swanson, A.A., et al., *Spinal Cord Ependymomas With MYCN Amplification Show Aggressive Clinical Behavior.* J Neuropathol Exp Neurol, 2019. **78**(9): p. 791-797.
34. Ghasemi, D.R., et al., *MYCN amplification drives an aggressive form of spinal ependymoma.* Acta Neuropathol, 2019. **138**(6): p. 1075-1089.
35. Yeboa, D.N., et al., *National Patterns of Care in the Management of World Health Organization Grade II and III Spinal Ependymomas.* World

Neurosurg, 2019.

36. Ruda, R., et al., *EANO guidelines for the diagnosis and treatment of ependymal tumors.* Neuro Oncol, 2018. **20**(4): p. 445-456.
37. Van der Auwera, G.A., et al., *From FastQ data to high confidence variant calls: the Genome Analysis Toolkit best practices pipeline.* Curr Protoc Bioinformatics, 2013. **43**: p. 11 10 1-11 10 33.
38. Wu, G., et al., *The genomic landscape of diffuse intrinsic pontine glioma and pediatric non-brainstem high-grade glioma.* Nat Genet, 2014. **46**(5): p. 444-450.
39. Rausch, T., et al., *DELLY: structural variant discovery by integrated paired-end and split-read analysis.* Bioinformatics, 2012. **28**(18): p. i333-i339.
40. da Silva, J.M., et al., *Genome-wide copy number variation (CNV) detection in Nelore cattle reveals highly frequent variants in genome regions harboring QTLs affecting production traits.* BMC Genomics, 2016. **17**: p. 454.
41. Talevich, E., et al., *CNVkit: Genome-Wide Copy Number Detection and Visualization from Targeted DNA Sequencing.* PLoS Comput Biol, 2016. **12**(4): p. e1004873.
42. Wang, W., et al., *Genome-wide detection of copy number variations among diverse horse breeds by array CGH.* PLoS One, 2014. **9**(1): p. e86860.
43. Zhang, H., et al., *Detection of genome-wide copy number variations in two chicken lines divergently selected for abdominal fat content.* BMC Genomics, 2014. **15**: p. 517.
44. Shim, S.R. and S.J. Kim, *Intervention meta-analysis: application and practice using R software.* Epidemiol Health, 2019. **41**: p. e2019008.
45. Zamecnik, J., et al., *Pediatric intracranial ependymomas: prognostic relevance of histological, immunohistochemical, and flow cytometric factors.* Mod Pathol, 2003. **16**(10): p. 980-91.
46. Kurt, E., et al., *Identification of relevant prognostic histopathologic features in 69 intracranial ependymomas, excluding myxopapillary ependymomas and subependymomas.* Cancer, 2006. **106**(2): p. 388-95.

47. Ho, D.M., et al., *A clinicopathologic study of 81 patients with ependymomas and proposal of diagnostic criteria for anaplastic ependymoma.* J Neurooncol, 2001. **54**(1): p. 77-85.
48. Gilbertson, R.J., et al., *ERBB receptor signaling promotes ependymoma cell proliferation and represents a potential novel therapeutic target for this disease.* Clin Cancer Res, 2002. **8**(10): p. 3054-64.
49. Verstegen, M.J., et al., *Proliferation- and apoptosis-related proteins in intracranial ependymomas: an immunohistochemical analysis.* J Neurooncol, 2002. **56**(1): p. 21-8.
50. Wolfsberger, S., et al., *Ki-67 immunolabeling index is an accurate predictor of outcome in patients with intracranial ependymoma.* Am J Surg Pathol, 2004. **28**(7): p. 914-20.
51. Armstrong, T.S., et al., *Adult ependymal tumors: prognosis and the M. D. Anderson Cancer Center experience.* Neuro Oncol, 2010. **12**(8): p. 862-70.
52. Xi, S., et al., *Clinical significance of the histological and molecular characteristics of ependymal tumors: a single institution case series from China.* BMC Cancer, 2019. **19**(1): p. 717.
53. Wu, T., et al., *Characterization of global 5-hydroxymethylcytosine in pediatric posterior fossa ependymoma.* Clin Epigenetics, 2020. **12**(1): p. 19.
54. Zhao, F., et al., *Survival and Prognostic Factors of Adult Intracranial Ependymoma: A Single-institutional Analysis of 236 Patients.* Am J Surg Pathol, 2021. **45**(7): p. 979-987.
55. Zawrocki, A., et al., *Analysis of the prognostic significance of selected morphological and immunohistochemical markers in ependymomas, with literature review.* Folia Neuropathol, 2011. **49**(2): p. 94-102.
56. Korshunov, A., et al., *Molecular staging of intracranial ependymoma in children and adults.* J Clin Oncol, 2010. **28**(19): p. 3182-90.
57. Figarella-Branger, D., et al., *Prognostic factors in intracranial ependymomas in children.* J Neurosurg, 2000. **93**(4): p. 605-13.
58. Horn, B., et al., *A multi-institutional retrospective study of intracranial ependymoma in children: identification of risk factors.* J Pediatr Hematol

Oncol, 1999. **21**(3): p. 203-11.

59. Antin, C., et al., *EZHIP is a specific diagnostic biomarker for posterior fossa ependymomas, group PFA and diffuse midline gliomas H3-WT with EZHIP overexpression.* Acta Neuropathol Commun, 2020. **8**(1): p. 183.
60. Johannessen, A.L. and S.H. Torp, *The clinical value of Ki-67/MIB-1 labeling index in human astrocytomas.* Pathol Oncol Res, 2006. **12**(3): p. 143-7.
61. Shivaprasad, N.V., et al., *Ki-67 immunostaining in astrocytomas: Association with histopathological grade - A South Indian study.* J Neurosci Rural Pract, 2016. **7**(4): p. 510-514.
62. Thotakura, M., N. Tirumalasetti, and R. Krishna, *Role of Ki-67 labeling index as an adjunct to the histopathological diagnosis and grading of astrocytomas.* J Cancer Res Ther, 2014. **10**(3): p. 641-5.
63. Pouget, C., et al., *Ki-67 and MCM6 labeling indices are correlated with overall survival in anaplastic oligodendroglioma, IDH1-mutant and 1p/19q-codeleted: a multicenter study from the French POLA network.* Brain Pathol, 2020. **30**(3): p. 465-478.
64. Wood, H., *Neuro-oncology: a molecular staging system for ependymoma.* Nat Rev Neurol, 2010. **6**(8): p. 414.
65. Hirose, Y., et al., *Chromosomal abnormalities subdivide ependymal tumors into clinically relevant groups.* Am J Pathol, 2001. **158**(3): p. 1137-43.
66. Dyer, S., et al., *Genomic imbalances in pediatric intracranial ependymomas define clinically relevant groups.* Am J Pathol, 2002. **161**(6): p. 2133-41.
67. Appay, R., et al., *CDKN2A homozygous deletion is a strong adverse prognosis factor in diffuse malignant IDH-mutant gliomas.* Neuro Oncol, 2019. **21**(12): p. 1519-1528.
68. Reis, G.F., et al., *CDKN2A loss is associated with shortened overall survival in lower-grade (World Health Organization Grades II-III) astrocytomas.* J Neuropathol Exp Neurol, 2015. **74**(5): p. 442-52.
69. Ma, S., et al., *Prognostic impact of CDKN2A/B deletion, TERT mutation, and EGFR amplification on histological and molecular IDH-wildtype glioblastoma.* Neurooncol Adv, 2020. **2**(1): p. vdaa126.

70. Lim, K.Y., et al., *ZFTA-YAP1 fusion-positive ependymoma can occur in the spinal cord: Letter to the editor.* Brain Pathol, 2022. **32**(1): p. e13020.
71. Lim, K.Y., et al., *Molecular subtyping of ependymoma and prognostic impact of Ki-67.* Brain Tumor Pathol, 2022. **39**(1): p. 1-13.